Prepared for submission to JHEP

Discovery reach for generic supersymmetry at the LHC: M_{T2} versus missing transverse momentum selections for pMSSM searches

Benjamin C. Allanach,[a] **Alan J. Barr,**[b] **Alexandru Dafinca**[b] **and Claire Gwenlan**[b]

[a] *University of Cambridge, DAMTP, Centre for Mathematical Sciences Wilberforce Road, Cambridge, CB3 0WA, United Kingdom*

[b] *University of Oxford, Sub-department of Particle Physics Denys Wilkinson Building, Keble Road, Oxford, OX1 3RH, United Kingdom*

E-mail: B.C.Allanach@damtp.cam.ac.uk, a.barr1@physics.ox.ac.uk, a.dafinca1@physics.ox.ac.uk, c.gwenlan1@physics.ox.ac.uk

Abstract: Different search strategies for supersymmetry have been employed by the LHC general-purpose experiments using early data. As proven by their early results, these strategies are promising, but raise the question of how well they will generalize for the future. We address this question by studying two thousand phenomenological minimal supersymmetric standard model parameter space points that come from a fit to indirect and cosmological data. We examine the 5σ discoverability of the points employing a typical ATLAS-type search based on missing transverse momentum (MET), a search based on an optimised M_{T2} cut and a combination of the two, taking into account standard model backgrounds. The discovery reach of the strategies can depend strongly on the systematic uncertainty in the background, subject to the stringency of the cuts and the details of the background simulation. By combining the MET and M_{T2} based strategies, with an integrated luminosity of 1 fb^{-1} (10 fb^{-1}) at 7 TeV, 4-8% (42%) of the points are discoverable, depending on the systematic uncertainty on the background. At 14 TeV and with 10 fb^{-1}, 96% of the points are discoverable. While the majority of points can be discovered by both strategies at $\sqrt{s} = 14$ TeV and with 1 fb^{-1}, there are some that are left undiscovered by a MET search strategy, but which are discovered by the M_{T2} strategy, and vice versa, therefore it is essential that one performs both in parallel. We discuss some of the factors that can make points more difficult to observe.

Keywords: Supersymmetry Phenomenology, Hadron Collider

ArXiv ePrint: 1105.1024

Contents

1 Introduction

The search strategies for supersymmetry at the LHC experiments ATLAS [1] and CMS [2] have been designed to be as general as possible. At the time of their design they were most extensively tested by the experiments in simulations on 7 and 14 benchmark points, respectively. These points are thought to be representative for whole extended regions in the minimal supersymmetric standard model (MSSM) parameter space, but in fact belong to one particular constrained model called mSUGRA/CMSSM. Therefore it is possible that these points do not cover all of the MSSM parameter space satisfactorily. The search strategies (for example cuts) have been optimized to increase the efficiency of the searches in these particular cases. It is important to understand to what extent these searches will be able to discover SUSY in other, less constrained regions of the MSSM parameter space.

The searches are based on the observation that in a wide range of SUSY models, squarks and gluinos are expected to cascade decay to jets, leptons or photons. The final state is expected to contain stable, weakly interacting (and therefore invisible) heavy particles, which make a good candidate for dark matter. These will escape detection, giving rise

to missing transverse momentum in the detector. SUSY searches at the LHC [3], [4] are heavily based on this signature, requiring large missing transverse momentum in order to discriminate standard model processes from supersymmetric events. In our paper, we call such a search a MET-based strategy.

Another strategy examined in this paper is incited by the fact that many well-motivated models of new physics have a Z_2 parity (for example R-parity in supersymmetry), which predicts that supersymmetric particles must be produced in pairs. Each of the two supersymmetric particles cascade decays within the detector to the lightest parity-odd particle, which is stable and assumed to be weakly interacting. R-parity therefore gives rise to very particular event topologies. The M_{T2} variable [5, 6] is a kinematic variable that uses experimentally measurable quantities (the missing transverse momentum being one of them) efficiently, by exploiting the topology of the event, to extract information about the masses of the produced particles. Search strategies using M_{T2} as a discriminating variable have been designed [7] and recently applied by the ATLAS experiment in [3].

The latest results from the ATLAS [3] and CMS [4] experiments have proven that their search strategies for supersymmetry are promising. However, we would like to understand how well these generalize to the future. Two recent studies [8, 9] have examined ATLAS MET based search strategies in a more general context by simulating signals for $\sim$ 71k model points within the phenomenological MSSM (pMSSM). The landscape of the pMSSM parameter space has also been explored in a study by AbdusSalam et al. [10], who have performed a global Bayesian fit of the pMSSM to current indirect collider and dark matter data. The parameters of the pMSSM were constrained in the fit, resulting in inferences on sparticle masses. In the present paper, we take a sample of points from the fit of reference [10] with a probability proportional to their posterior probability function. Extending the work of [8, 9], which do not examine the discovery reach of M_{T2} based searches, in this paper we will use the points sampled from reference [10] to:

- determine how likely not only MET-based searches, but also M_{T2}-based searches are to discover SUSY.
- understand the successes and failures of the searches.
- optimise the searches for the more general pMSSM scenario.

The plan of this report is as follows. First we give a short account of the properties of the SUSY points examined, sampled by [10]. Then, the MET and M_{T2} based search strategies and the corresponding event selection are explained in sections 3 and 4. We briefly present in section 5 the technicalities of simulating the events for different model points, a basic detector simulation, a discussion of the Standard Model backgrounds and provide a definition of *discoverability*. Section 6 shows how the SUSY discoverability varies with the choice of the M_{T2} cut for different centre of mass energies (7 and 14 TeV) and a variety of integrated luminosities, in the context of a search strategy based on M_{T2} alone and a combined search strategy based on both MET and M_{T2}. We discuss the most recent ATLAS exclusion limits on sparticle masses and compare them with the expectations from our study in section 7. The effect of systematic uncertainties in the background on

discoverability is detailed in section 8. Optimal cuts are proposed in section 9. We discuss what makes a point difficult to discover in section 10. Finally, section 11 contrasts our work on the M_{T2} search strategy with the analysis from references [8, 9] performed on other ATLAS MET-based search strategies. We conclude in section 12.

2 Points investigated

A total of 1940 points were provided by the authors of [10]. They are sampled from the posterior probability distribution obtained through a Bayesian fit of electroweak, search and flavour physics data to the pMSSM. The pMSSM contains the most relevant 25 weak-scale MSSM parameters. The priors used in the analysis are flat in mass parameters except for the scalar mass parameters, which are flat in the logarithm. Inferences are made about these points without assuming a restrictive high-scale supersymmetry breaking model. The

Parameter	Allowed range
Scalar masses	$[100\ \text{GeV}, 4\ \text{TeV}]$
Trilinear scalar coupling	$[-8\ \text{TeV}, 8\ \text{TeV}]$
Gaugino masses	$[-4\ \text{TeV}, 4\ \text{TeV}]$
$\tan\beta$	$[2, 60]$

Table 1: Allowed ranges for the pMSSM parameters. $\tan\beta$ is the ratio of the MSSM Higgs vacuum expectation values.

ranges of allowed values for some of the parameters are summarized in table 1. Five of the 25 pMSSM parameters varied were associated with the Standard Model: the top mass, the mass of the Z boson, the bottom quark mass and the strong coupling constant. The relic density of dark matter inferred from cosmological measurements proved to be the most important constraint. Various observables involving bottom quarks were used to constrain the model: the branching ratios of $B_S \to \mu^+\mu^-$, $B_u \to \tau\nu$ and $B \to X_s\gamma$ as well as the $B_s - \bar{B}_s$ mass difference and the $B \to K^*\gamma$ isospin asymmetry. The electroweak observables used were: the W boson mass, the mass and decay width of the Z boson, the effective weak mixing angle, $Z-$pole asymmetry parameters and the muon anomalous magnetic moment. Direct pre-LHC searches for sparticles and Higgs bosons were also used. The 25 dimensional parameter space was successfully scanned with the `MultiNest` algorithm [11, 12], achieving a statistically convergent fit. The resulting fit was far from being robust, since there were not enough data to constrain so many parameters, and this manifests itself in the high degree of prior dependence in the results. In the present paper, we are not concerned with the issue of fit robustness: we merely want to use a subset of the points that fit current data well in order to investigate the properties of proposed search strategies in a general context, as explained in Section 1.

Together with the SPS1a point [13], these points form the pool of scenarios studied in this report. A flavour of their mass spectra is given in figure 1. In the sampling from the pMSSM, the physical masses of the sparticles was constrained to lay below 4 TeV. In

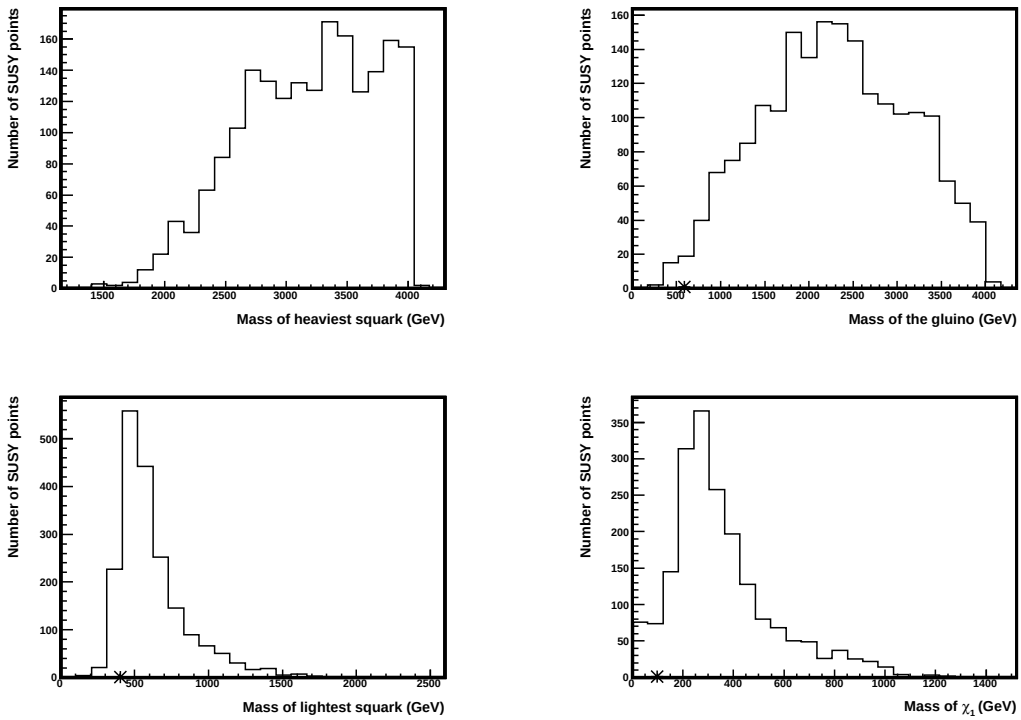

Figure 1: A flavour of the mass spectra of the 1941 SUSY points investigated. The * denotes the SPS1a point. A * is missing from the first histogram since the heaviest squark of the SPS1a point ($m = 586$ GeV) is much lighter than the corresponding squark in any of the other points examined.

contrast, all seven mSUGRA/CMSSM benchmark points used by the ATLAS collaboration in [14] have a gluino mass below 1 TeV. Notice that the SPS1a point, which is used widely as a benchmark point, is also in the low mass end of the spectra and is now excluded by the ATLAS experiment [3].

3 MET based search strategy

The final state of supersymmetric events is expected to contain stable, weakly interacting (and therefore invisible) heavy particles. These will escape detection, giving rise to missing transverse momentum in the detector. In this paper we study one possible discovery channel, in which we require 4 or more jets and 0 leptons in the final state. The 0 lepton requirement suppresses the (semi)leptonic decays of W, Z and $t\bar{t}$, whereas the large number of jets suppresses the QCD background. The concrete selection for this channel follows the recipe laid out in [1]. We require:

- at least four jets with transverse momentum $p_T > 50$ GeV, at least one jet must have $p_T > 100$ GeV
- missing transverse momentum $\not{p}_T > 100$ GeV

- no isolated leptons with $p_T > 20$ GeV
- the smallest azimuthal separation between the jet direction and the missing transverse momentum, $\Delta\phi\left(\text{jet}_i, \not{\mathbf{p}}_T\right) > 0.2$ for the first three jets
- effective mass $M_{\text{eff}} > 800$ GeV
- $\not{p}_T > 0.2\ M_{\text{eff}}$
- transverse sphericity $S_T > 0.2$

The missing transverse momentum $\not{\mathbf{p}}_T$ is calculated as the negative sum of the transverse momenta of all visible objects within detector acceptance:

$$\not{\mathbf{p}}_T \equiv -\sum_i \mathbf{p}_T{}^{(i)} \tag{3.1}$$

where we define the acceptance as having pseudorapidity $|\eta| < 5$ and only take into account objects with $p_T > 0.5$ GeV.[a]

The effective mass M_{eff} is defined as the scalar sum of transverse momenta of the most energetic objects in the event - in this case four jets, together with the missing transverse momentum:

$$M_{\text{eff}} \equiv \sum_{i=1}^{n=4} \left|\mathbf{p}_T{}^{(i)}\right| + \not{p}_T \tag{3.2}$$

The transverse sphericity S_T is defined as:

$$S_T \equiv \frac{2\lambda_2}{(\lambda_1 + \lambda_2)} \tag{3.3}$$

with λ_1 and λ_2 being the eigenvalues of the 2×2 sphericity tensor $S_{ij} = \sum_k \left(p_T^{(k)}\right)_i \left(p_T^{(k)}\right)_j$. The tensor is computed using all jets with $|\eta| < 2.5$ and $p_T > 20$ GeV.

A simplified version of this strategy, suitable for early data, was employed by ATLAS for three of the four signal regions defined in reference [3]. These follow the same philosophy as reference [1], but require a reduced jet multiplicity and slightly looser cuts to suit the limited statistics. The fourth signal region of reference [3] employed a different selection variable described in the following section.

4 M_{T2} based search strategy

The M_{T2} variable is a generalization of the transverse mass to the case of decays of pairs of particles [5, 6]. Each of the two decays will contribute to the final state with one visible and one invisible object. The transverse momentum $\mathbf{p}_T{}^{(1)}$ and $\mathbf{p}_T{}^{(2)}$ of each of the visible objects can be measured in the detector. However, only the *total* transverse momentum of the invisible objects can be measured as missing transverse momentum $\not{\mathbf{p}}_T$. Nevertheless,

[a] $\eta = -\ln\left[\tan\left(\frac{\theta}{2}\right)\right]$, where θ is the angle between the particle 3-momentum and the beam axis.

for each of the decays labeled by $i = 1, 2$ one can compute the transverse mass $m_T^{(i)}$ under the assumption of a massless invisible object:

$$m_T^{(i)^2}(\mathbf{p}_T{}^{(i)}, \not{\mathbf{q}}_T{}^{(i)}) \equiv 2\left|\mathbf{p}_T{}^{(i)}\right|\left|\not{\mathbf{q}}_T{}^{(i)}\right| - 2\mathbf{p}_T{}^{(i)} \cdot \not{\mathbf{q}}_T{}^{(i)} \tag{4.1}$$

where $\not{\mathbf{q}}_T{}^{(i)}$ is a guess for the true, unknown missing transverse momentum $\not{\mathbf{p}}_T{}^{(i)}$. The variable M_{T2} is defined by:

$$M_{T2}(\mathbf{p}_T{}^{(1)}, \mathbf{p}_T{}^{(2)}, \not{\mathbf{p}}_T) \equiv \min_{\sum \not{\mathbf{q}}_T = \not{\mathbf{p}}_T} \left\{\max\left(m_T^{(1)}, m_T^{(2)}\right)\right\} \tag{4.2}$$

The minimization takes place over all values of the two undetectable particles' possible missing transverse momenta $\not{\mathbf{q}}_T{}^{(1,2)}$ consistent with the constraint $\sum \not{\mathbf{q}}_T = \not{\mathbf{p}}_T$.

The variable M_{T2} gives the greatest lower bound on the parent mass for a given event that is consistent with the observed momenta and hypothesised masses [15]. When plotted over all events with the same parent particles, one expects an endpoint to appear. For example, for $t\bar{t}$ production, we expect M_{T2} to have an endpoint at the mass of the top quark. While the endpoint will be smeared by effects such as detector resolution, simulations [7] show that the vast majority of standard model background events have $M_{T2} < m_t$. For SUSY events however, where the actors are far heavier particles, one can expect M_{T2} to have larger values. This allows good discrimination between signal and background for the region $M_{T2} > m_{\text{top}}$.[b] Motivated by this observation, the use of the M_{T2} variable as a complement to the standard ATLAS search strategies has been advocated in [7] and is now being actively pursued by the ATLAS collaboration, for example in [3, 16].

Typical M_{T2} spectra for simulated backgrounds and for the SPS1a SUSY scenario are displayed in figure 2, reproducing results of [7]. These were obtained as described in section 5. The figure shows that for a M_{T2} cut $\gtrsim 600$ GeV placed too high, not only the background, but also the signal is suppressed. For values of the M_{T2} cut too low, the background swamps the signal. Our goal is to strike a balance between these two extremes. Based on the SPS1a point one can find the range of values for a cut on M_{T2} which will render the SPS1a model discoverable, i.e. which 1) provides a sufficient number of signal events after selection and 2) provides a small enough p – value for the background-only hypothesis. The meaning of "sufficient number" and "small enough" will be defined in the next section. SPS1a is only one possible scenario of how nature could look, so when determining the optimal value for the cut on M_{T2}, we perform the same analysis on many other scenarios.

ATLAS has implemented in one of the four signal regions in reference [3] an M_{T2} search strategy by requiring no leptons, a jet multiplicity $\geq$ two, with the leading jet $p_T > 120$ GeV, second jet $p_T > 40$ GeV, $\not{p}_T > 100$ GeV, $\Delta\phi\left(\text{jet}, \not{\mathbf{p}}_T\right) > 0.4$ and $M_{T2} > 300$ GeV. The M_{T2} variable is calculated using the two highest-p_T jets. The $\not{p}_T$ requirement makes an effective trigger, while the $\Delta\phi$ requirement reduces the QCD background.

In this paper we take a simplified version of this analysis, with the intention of examining the effect of a cut on M_{T2} alone. We only require two or more jets with $p_T > 50$ GeV,

[b] We note that for fairly degenerate mass spectra, where the splitting between sparticles is less than the top mass, good discrimination may not be possible.

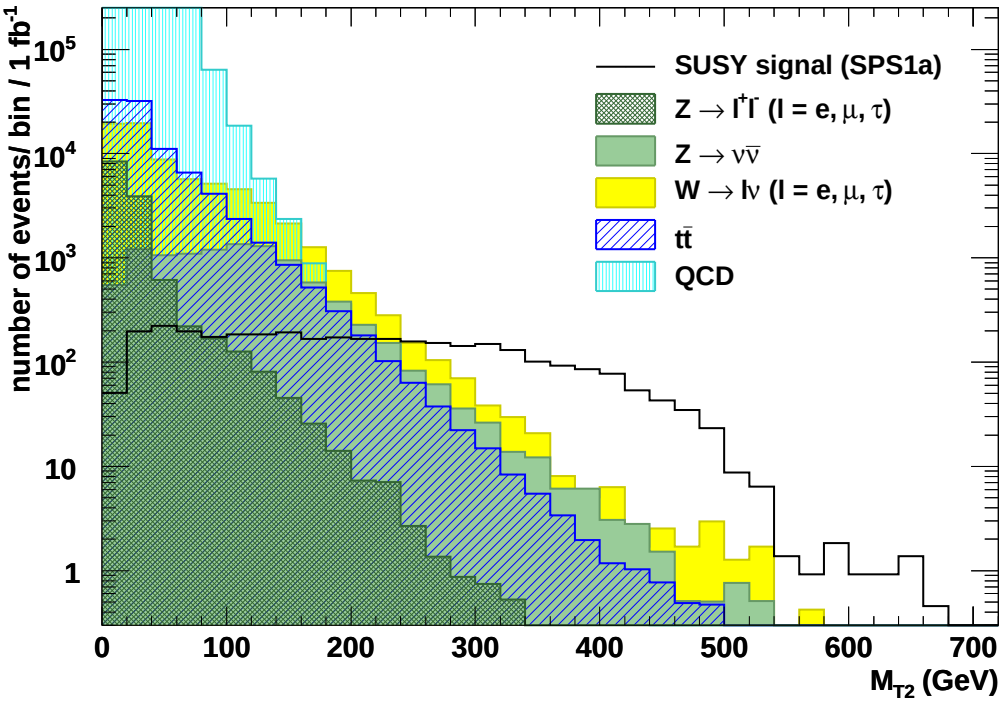

Figure 2: Distribution of M_{T2} for events with two or more jets with $p_T > 50$ GeV (and no other cuts) for an integrated luminosity of 1 fb^{-1} at $\sqrt{s} = 7$ TeV.

compute M_{T2} using the two highest-p_T jets and then cut at different values of M_{T2}. We call the value of M_{T2} at which the cut is set M_{T2}^{cut}. No restriction is set on the number of leptons.

5 Technical details

The following operations have been performed in this analysis:

- The spectrum information for each of the 1940 pMSSM points sampled by the authors of [10] and for the SPS1a point was passed to `Herwig++ 2.4.2` [17, 18] via the SUSY Les Houches Accord [19]. For each point we simulated 10 000 inclusive SUSY events. A sample of background events was produced, containing 10^7 events of each $t\bar{t}$, $W \to l\nu + \text{jets}$, $Z \to l^+l^- + \text{jets}$, $Z \to \nu\bar{\nu} + \text{jets}$. For QCD we produced 10^7 events for each slice of p_T of hard scatter, where the slices lie between 17, 35, 70, 140, 280, 560, 1120 GeV, with the last slice starting at 2240 GeV. This is to ensure we have sufficient simulated events at high p_T. The contribution from diboson+jets is expected to be very small according to [1]. For each of the SUSY scenarios and the background, we further performed the following:

- For each event, we clustered hadrons with fiducial pseudorapidity ($|\eta| < 5$) and momentum ($p_T > 0.5$ GeV) into jets using the fastjet [20] implementation of the anti-k_T

algorithm [21]. The E combination scheme with $R = 0.4$ and ${p_T}^{\min} = 10$ GeV was used.

- We simulated the effect of the detector in a simplified way by smearing the energy and momenta of the jets using a Gaussian probability function for the majority of $(1-\epsilon)$ events. The width of the Gaussian depends on the energy of the jet such that:

$$\sigma(E)/E_j = \left(0.36/\sqrt{E_j\,[\text{GeV}]}\right) \oplus 0.1 \tag{5.1}$$

where E_j is the unsmeared jet energy. This resolution is typical of general-purpose LHC detectors [1, 2]. The distribution also has a low energy tail to account for the possibility of badly mismeasured jets, therefore the remaining fraction $\epsilon = 1\%$ of the jets is smeared with a probability density:

$$\log P(r) = \begin{cases} c_1 r + c_2 & \text{for } (0.2 < r < 0.8) \\ 0 & \text{elsewhere} \end{cases} \tag{5.2}$$

where $r \equiv E/E_j$ is the ratio of the smeared jet energy to the true jet energy. The constant c_1 is chosen such that the resulting smearing function of a jet of given energy agrees with full simulation results as in [1] and c_2 is a normalization constant.

The missing transverse momentum is calculated from the negative vector sum of the jet momenta (after smearing) and other isolated particles present.

In addition, for the MET and M_{T2} search strategy individually, we determined the number of events passing the cuts defined in sections 3 and 4. For the M_{T2} based strategy we allowed for a variable cut on M_{T2}. We then compared the number of signal events with the number of background events to determine whether the point in question would be discoverable at a given luminosity. For a SUSY point to be *discoverable*, we require on one hand at least 10 SUSY events to pass the cuts. On the other hand, the signal should be well above background, i.e. the p – value for the background-only hypothesis should be low enough. We will convert the p – value into an equivalent significance Z, defined such that a Z standard deviation upward fluctuation of a Gaussian random variable would have an upper tail area equal to p. That is, $Z = \Phi^{-1}(1-p)$, with Φ being the cumulative distribution of the Standard Gaussian. We then require for a discovery that $Z > 5$. We can include the systematic uncertainty in the background by using the methods from reference [22].

Having decided for each SUSY point individually for which range of M_{T2}^{cut} it would be discoverable and whether the MET search strategy would discover the point, we would like to know the answers to the following questions:

- What is the overall optimal value for M_{T2}^{cut}?
- How is the optimal value of M_{T2}^{cut} affected as we include systematic uncertainties in the background?

- How is the optimal value of $M_{T2}^{\rm cut}$ affected as the experiments accumulate more luminosity?

- How does the optimized M_{T2} search compare to the MET search when taking into account the above?

We will address these questions in the following sections.

6 $\int \mathcal{L}dt$-dependent discoverability

At the time of writing, the LHC is scheduled to run at $\sqrt{s} = 7$ TeV, where it is planned to accumulate a total of a few fb^{-1}. Figure 3a shows the number of points discoverable with different luminosities at 7 TeV as a function of $M_{T2}^{\rm cut}$. For each integrated luminosity, two lines of the same style were drawn. The lower one shows the number of points discoverable with the M_{T2} based search strategy alone. The upper of the two lines with the same style shows discoverability for a combination of the M_{T2} and MET based strategies, where a point is considered to have been discovered if it was discovered by *either* the M_{T2} or the MET-based strategy. The flat sections of the upper lines give the number of points discoverable with the MET based search strategy alone. If no points were discovered with the MET based strategy, the M_{T2} only and combined strategy lines overlap. Only the histograms corresponding to an integrated luminosity of up to 1 fb^{-1} have been or will be experimentally explored with a center-of-mass energy of 7 TeV.

The same study can be applied for the LHC at its design center of mass energy of 14 TeV. Figure 3b shows the discoverability in this scenario. Due to the increased center of mass energy, high discoverability is achieved with far lower integrated luminosity.

Notice in figure 2 that our background sample is statistics limited at the high M_{T2} end, giving rise to a ragged, discontinuous spectrum. This translates in figures 3a-3d into possibly fake peaks of discoverability at large M_{T2} values. Therefore, one should view critically predictions of discoverability for $\sqrt{s} = 7$ (14) TeV for values of $M_{T2}^{\rm cut}$ above 520 GeV (780 GeV).

Once the discoverability profile and an optimal $M_{T2}^{\rm cut}$ value is found through simulations for a given integrated luminosity, it is not necessarily obvious if the same profile or optimal $M_{T2}^{\rm cut}$ value will apply for different luminosities. In the limit of large numbers of events and no systematic uncertainties in the background, the significance varies as $\propto \sqrt{\mathcal{L}}$. This implies that as more luminosity is accumulated, discoverability will increase at low $M_{T2}^{\rm cut}$ values, where high background is a problem for the significance. At the high $M_{T2}^{\rm cut}$ end, discoverability is not necessarily limited by the significance as much as by the fact that not enough signal events will have been recorded. Higher integrated luminosity increases discoverability for very high $M_{T2}^{\rm cut}$ values as well, since the number of signal events is proportional to luminosity. Considering these two effects together, we expect the "peak" of the discoverability distribution with respect to $M_{T2}^{\rm cut}$ to broaden and to shift to higher M_{T2} values. This explains the very flat maximum observed at high luminosity in figures 3a and 3b. One can choose a low M_{T2} value which optimizes the search at low luminosity - the flat

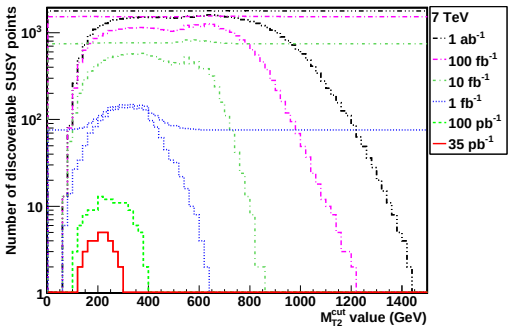

(a) $\sqrt{s} = 7$ TeV. Systematic uncertainties in the background have been neglected.

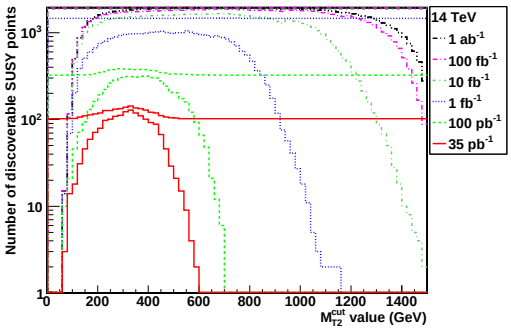

(b) $\sqrt{s} = 14$ TeV. Systematic uncertainties in the background have been neglected.

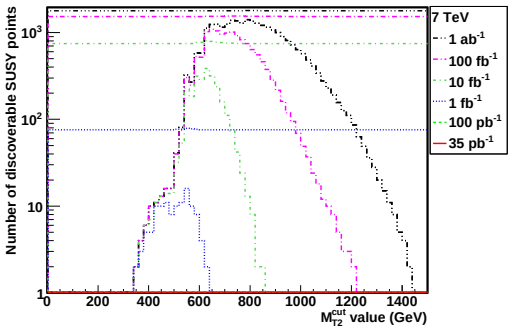

(c) $\sqrt{s} = 7$ TeV. The systematic uncertainty in the background was assumed to be 50%. Notice no points can be discovered with 35 pb^{-1}

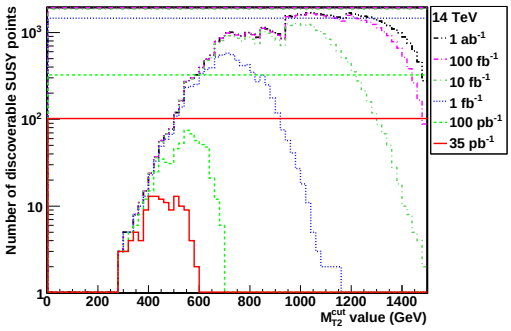

(d) $\sqrt{s} = 14$ TeV. The systematic uncertainty in the background was assumed to be 50%.

Figure 3: Number of SUSY points (out of 1941) discoverable at $\sqrt{s} = 7$ or 14 TeV versus $M_{T2}^{\rm cut}$ (bins of 20 GeV) for the M_{T2} based strategy (lower line of same style) and the combined strategy based on M_{T2} and MET (upper line of same style). For $\sqrt{s} = 7$ (14) TeV, predictions in the region above 520 (780) GeV might not be accurate due to the limited statistics in the background.

maximum will ensure that the same value will provide a nearly optimal strategy at higher luminosity as well.

We have studied discoverability by incrementing the luminosity by a factor of 10 each time. However, this does not buy nearly the same factor in discoverability. This is understandable since on one hand $Z \propto \sqrt{\mathcal{L}}$ at the optimal value of $M_{T2}^{\rm cut}$. On the other hand, if $\sqrt{s} < 2m_{\rm LSP}$, where $m_{\rm LSP}$ is the mass of the lightest supersymmetric particle, then sparticles are simply not produced, regardless of the luminosity.

From the corresponding discoverability plots it becomes apparent that, in the absence of uncertainties in the background, the optimized M_{T2} based strategy is better suited than the MET based strategy for integrated luminosities up to several inverse femtobarns, after which the MET based strategy performs better.

In an attempt to explain this, we found that the MET based search is too stringent and does not allow any background events at all and only very few signal events through. Therefore there are plenty of SUSY points which have fewer than 10 signal events passing the cuts of the MET based strategy. For these points, the discoverability is limited by the *number* of events, which grows linearly with the luminosity. On the other hand, the M_{T2} based strategy operating at the value of M_{T2}^{cut} giving maximal discoverability is *significance* limited and Z grows $\propto \sqrt{\mathcal{L}}$.

At low luminosity, not enough signal events pass cuts for the MET based strategy to be efficient. With increasing luminosity, the MET based strategy starts to dominate due to the linear growth of the number of events as opposed to the $\propto \sqrt{\mathcal{L}}$ growth of significance for the M_{T2} based strategy. At high luminosity, of more than a few inverse femtobarns, this effect is so evident that the combination of the M_{T2} and MET based strategies only discovers very few points more than the MET based strategy.

Figure 4 makes clear that while both the M_{T2} and MET based strategies are good at discovering a large sub-space of the pMSSM, at high luminosities above 1 fb^{-1} the MET based strategy explores the region of heavy gluino masses, $m_{\tilde{g}} \gtrsim 2$ TeV, more effectively. Whilst the two strategies have a large overlap of points they discover, there still are regions in the $(m_{\tilde{g}} - m_{\text{lightest } \tilde{q}})$ plane which are only explored by one or the other strategy. There are a variety of reasons for this, which include the inability to set a single cut threshold on M_{T2} which is optimal for all points and the relative sensitivity of each strategy to different jet multiplicities, jet p_T and decay topologies. As an example of such a reason, we note that the M_{T2} based strategy was designed for the topology of pair-producing SUSY particles, whose direct decays are assumed to produce the hardest two jets in the event. These are the jets that ought to enter the calculation of M_{T2}. However, we found it is possible for one or both of the two hardest jets in certain events to be initial or final state radiation. These events will be more likely to fail the M_{T2} than the MET cuts. Similarly, points favoring event topologies where the hardest two jets are daughters of SUSY particles will be discovered with the M_{T2} based strategy more easily. Since the the two strategies are predominantly accepting events of different topologies, a combined strategy tends to be more powerful than the individual strategies.

We conclude this section by noting that so far the LHC SUSY searches [3, 4] have not been strongly affected by multiple in-time pp collisions. In the future, due to the increase in the instantaneous luminosity, the effects of such pile-up will have to be investigated in dedicated studies, to include the modified response of the detector.

7 Exclusion limits from ATLAS

Turning the problem around, we ask: could one have expected the LHC to exclude SUSY at 95% confidence level (had it been one of the points in this study), with the integrated luminosity it achieved by the end of 2010, i.e. ~ 35 pb^{-1} and ignoring systematic uncertainties? The most stringent constraints up to now come from the ATLAS collaboration, which excludes in reference [3] at the 95% confidence level (CL) points with gluino or squark masses

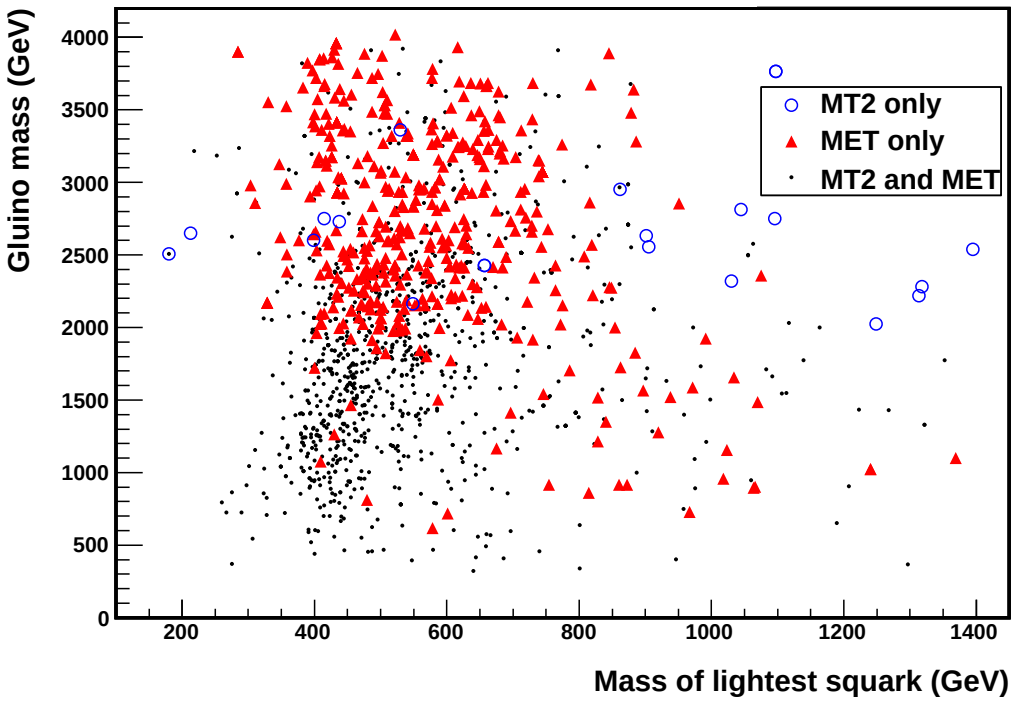

Figure 4: Points in the $(m_{\tilde{g}} - m_{\text{lightest } \tilde{q}})$ - plane, discovered by either M_{T2} alone, or MET alone, or by both MET and M_{T2}, assuming $\sqrt{s} = 14$ TeV, a luminosity of 1 fb^{-1} and a fixed systematic uncertainty in the background of 10%. The M_{T2} search operates at its optimum, which for this luminosity and systematic uncertainties is at M_{T2}^{cut}= 660 GeV.

up to 500 GeV in simplified models containing only squarks of the first two generations, a gluino octet and a massless neutralino.

For an M_{T2}^{cut} value between 200 and 240 GeV (which is our optimal value at the given luminosity) the combined strategy from this paper (after an integrated luminosity of 35 pb^{-1}) would have provided evidence for discovery with p – value $< 5\%$ for 54 points, including the SPS1a point. These points should have been discovered or excluded at 95% CL by the LHC experiments in references [3, 4]. Indeed, these 54 points have squark and gluino masses that fall within the exclusion limits of the simplified model of the ATLAS analysis [3]. The simplified model assumed $m_{\tilde{\chi_1}} = 0$, which is the value for which discovery would be most straightforward, and contain no other light supersymmetric particles. Whilst it is true that our 'discoverable' model points all have $(m_{\text{lightest } \tilde{q}}, m_{\tilde{g}})$ values which lie within the exclusion region of the ATLAS analysis, the inverse is not true; there are many points in the sample examined in this paper with *squark and gluino masses* that lie within the ATLAS simplified-model exclusion region which would *not* be discovered with 35 pb^{-1} – for a variety of different reasons. Some characteristic sparticle masses of the five points which need least luminosity for exclusion are shown in table 2. The characteristics of some of the points that are found to be most difficult to discover with 10 fb^{-1} at $\sqrt{s} = 14$ TeV are

discussed in section 10. The points studied therein do not fall within the ATLAS exclusion region, but the reasons for which they are difficult to discover also apply to the elusive points lying within the ATLAS exclusion region.

Point	$m_{\tilde{g}}$ (GeV)	Mass of lightest squark from the first two generations (GeV)	Mass of lightest squark from the third generation (GeV)	m_{χ_1}(GeV)
n65	520	395 ($\tilde{u}_L, \tilde{u}_R, \tilde{c}_L, \tilde{c}_R$)	848 ($\tilde{b}_1$)	229
n188	560	430 ($\tilde{d}_R, \tilde{u}_L, \tilde{s}_R, \tilde{c}_L$)	437 ($\tilde{b}_1$)	198
SPS1a	604	548 ($\tilde{d}_R, \tilde{u}_R, \tilde{s}_R, \tilde{c}_R$)	401 ($\tilde{t}_1$)	97
p29	597	406 ($\tilde{u}_L, \tilde{c}_L$)	1955 ($\tilde{t}_1$)	183
p780	546	398 ($\tilde{u}_L, \tilde{c}_L$)	306 ($\tilde{b}_1$)	199

Table 2: SUSY points that would have been excluded or discovered at 5σ with $\int \mathcal{L}dt = 35$ pb^{-1} at $\sqrt{s} = 7$ TeV with a combination of the M_{T2} and MET based search strategies as described in this paper. In two of the columns we show in parentheses the lightest squark flavour belonging to the first two or the third generation. For the case of the first two squark generations, we group together several squarks with near-degenerate masses if their mass difference is less than 1 GeV.

8 Including systematic uncertainties

Unavoidably, there will be both theoretical and experimental uncertainties in the background. We model the uncertainties in the background by assuming a conservative systematic uncertainty of 50%, which is comparable to that reported for signal regions B and D in the latest ATLAS SUSY search [3].

For the study of the effect of systematic uncertainties we assume the background to be a Poisson process with mean $\hat{b}$, where $\hat{b}$ itself is a Gaussian-distributed quantity with a standard deviation of max $\left\{50\% \times \hat{b}, 1 \text{ event}\right\}$. For each SUSY point we calculate in bins of M_{T2}^{cut} the p – value for the background-only hypothesis, which again can be translated into a significance as described in reference [22]. With the altered prescription for calculating the significance, the discoverability is changed to the one displayed in figures 3c and 3d. The intermediate regime of a systematic uncertainty in the background of 10% is also considered in this study. The effect of including the systematic uncertainties in the background is to push up the optimal value of M_{T2}^{cut}.

Assuming a constant fraction of 50% systematic error in the background, regardless of the value of M_{T2}^{cut}, is a rather naïve assumption. However, the detailed determination of the uncertainties in the backgrounds will require both complete detector simulation and supporting measurements from the LHC data, and so can only be performed by the experimental collaborations themselves. Our assumptions on the uncertainties should not affect the qualitative discussion we present in this paper, however.

9 Optimal $M_{T2}^{\rm cut}$

We will consider the optimal value of the M_{T2} cut to be the one which maximizes the number of discoverable points according to the two conditions outlined in section 5. These conditions take into account both statistical and systematic uncertainties. For the optimum determination we have calculated the number of discoverable points in bins of the $M_{T2}^{\rm cut}$ in sections 6 and 8 and found the bin with the most entries.

There are two caveats linked to our determination of the optimum, neither of which is directly relevant for the experimental measurements. Firstly, our optimal $M_{T2}^{\rm cut}$ is based on the limited number of events that we have simulated in the tail of the M_{T2} distribution for both signal and background. Secondly, the overall systematic uncertainty will vary across the space of the selection variables, whereas we have assumed it to be constant. What will be done in practice by the experiments will be to determine most of the backgrounds and their uncertainties from other measurements of LHC data.

Table 3 summarizes the results for the optimal $M_{T2}^{\rm cut}$ value in the cases of no systematic uncertainty in the background, or an assumed 10% or 50% systematic uncertainty. The general trend is that the optimal value of $M_{T2}^{\rm cut}$ goes up with increasing luminosity, as expected from the discussion in section 6. In figure 3b we observe that the maximum of discoverability is very flat in $M_{T2}^{\rm cut}$, such that choosing an $M_{T2}^{\rm cut}$ value which maximizes discoverability at say 100 pb^{-1} will be approximately optimal for higher luminosities as well. Considering the above, the following values look reasonable for the choice of the initial $M_{T2}^{\rm cut}$ value for low luminosities, in the context of a combination of the M_{T2} and MET based search strategies: for running at 7 TeV, 320 GeV; for running at 14 TeV, 400 GeV.

We also notice that with 50% uncertainty in the background, the M_{T2} based strategy barely adds any discoverability to the MET results.

10 Difficult points

Some difficult SUSY points evade detection unless they are tackled with a high energy LHC with high luminosity. Why is this the case? There are in principle two types of reasons:

- The sparticle masses are very large with a consequently low SUSY production cross-section;
- The mass spectrum and branching ratios lead to decay topologies / kinematics with low values of the variables which the search strategies cut on.

Reasons of the first type need to be tackled with higher center-of-mass energies and higher luminosities. Reasons of the second type need to be tackled by improving the search strategies. Figure 5 sheds light over which of the two types of reasons dominate discoverability for the SUSY points investigated. It shows points in the ($m_{\tilde{g}}$, $m_{\rm lightest\,\tilde{q}}$) plane, color-coded to describe the luminosity needed for discovery in the scenario of $\sqrt{s} = 14$ TeV with a combination of the MET based and the optimized M_{T2} based search strategy and

Energy		7 TeV			14 TeV		
Background uncertainty $\sigma_{\hat{b}}/\hat{b}$ =		0%	10%	50%	0%	10%	50%
$\mathcal{L} = 35$ pb^{-1}	M_{T2}	0.3%	0.2%	0.0%	6.6%	4.6%	0.7%
	MET	0.0%	0.0%	0.0%	5.3%	5.3%	5.3%
	combined	0.3%	0.2%	0.0%	7.4%	6.2%	5.3%
$\mathcal{L} = 100$ pb^{-1}	M_{T2}	0.7%	0.5%	0.1%	16.3%	12.5%	3.9%
	MET	0.0%	0.0%	0.0%	16.7%	16.7%	16.7%
	combined	0.7%	0.5%	0.1%	19.9%	17.6%	16.8%
$\mathcal{L} = 1$ fb^{-1}	M_{T2}	7.2%	4.1%	0.8%	54.3%	47.6%	29.7%
	MET	3.9%	3.9%	3.9%	75.2%	75.2%	75.2%
	combined	7.7%	5.4%	4.1%	76.2%	76.2%	75.4%
$\mathcal{L} = 10$ fb^{-1}	M_{T2}	29.9%	26.1%	19.8%	85.8%	81.6%	65.2%
	MET	38.4%	38.4%	38.4%	95.9%	95.9%	95.9%
	combined	42.5%	42.5%	41.6%	96.1%	96.0%	96.0%
$\mathcal{L} = 100$ fb^{-1}	M_{T2}	(65.0%)	(64.6%)	(56.2%)	96.2%	92.7%	85.4%
	MET	(78.8%)	(78.8%)	(78.8%)	99.5%	99.5%	99.5%
	combined	(80.3%)	(80.3%)	(80.0%)	99.6%	99.6%	99.6%
$\mathcal{L} = 1$ ab^{-1}	M_{T2}	(82.6%)	(80.3%)	(72.6%)	99.0%	95.9%	87.2%
	MET	(91.6%)	(91.6%)	(91.6%)	99.8%	99.8%	99.8%
	combined	(92.2%)	(92.2%)	(92.1%)	99.9%	99.9%	99.9%

Table 3: Percentage of discoverable points (out of 1941) for the optimised M_{T2} based, the MET based and the combined search strategies, different luminosities and $\sqrt{s} = 7,\ 14$ TeV. The systematic uncertainty in the background is taken to be a fixed percentage, $f = 0\%$, 10% or 50% of the expected number of background events $\hat{b}$, but at least one event, i.e. $\sigma_{\hat{b}} = \max\left\{f \times \hat{b} \text{ events}, 1 \text{ event}\right\}$. The entries in brackets show the fractions of discoverable points for luminosities which we do not expect to be recorded at those energies. The number of points discovered with our MET based strategy does not depend on the systematic uncertainty in the background due to none of the simulated background events passing the stringent cuts of this analysis. A more careful analysis [8, 9] of the expected backgrounds shows a strong dependence of discoverability on the size of the systematic uncertainty.

ignoring systematic uncertainties in the background. The value $M_{T2}^{\text{cut}} = 320$ GeV optimizes the cut "in the long run", i.e. for 1 fb^{-1} and above. The points which are hard to discover predominantly populate high-mass regions of the ($m_{\tilde{g}}$, $m_{\text{lightest } \tilde{q}}$) plane. The transition from black (easily discoverable with ~ 1 pb^{-1}) in the bottom left corner to yellow[c] (hard to discover, need > 10 fb^{-1}) at the extremities does not seem to be single-valued and figure 6 examines this further. It shows the luminosity needed for discovery in the (Δm, $m_{\text{lightest sparton}}$) plane, with Δm being the difference between the mass of the lightest sparton and that of the LSP. Figure 6 shows that the heavier the sparticles, the harder it is to discover the point the sparticles belong to. However, for the same mass value for

[c] light gray in a b/w printout

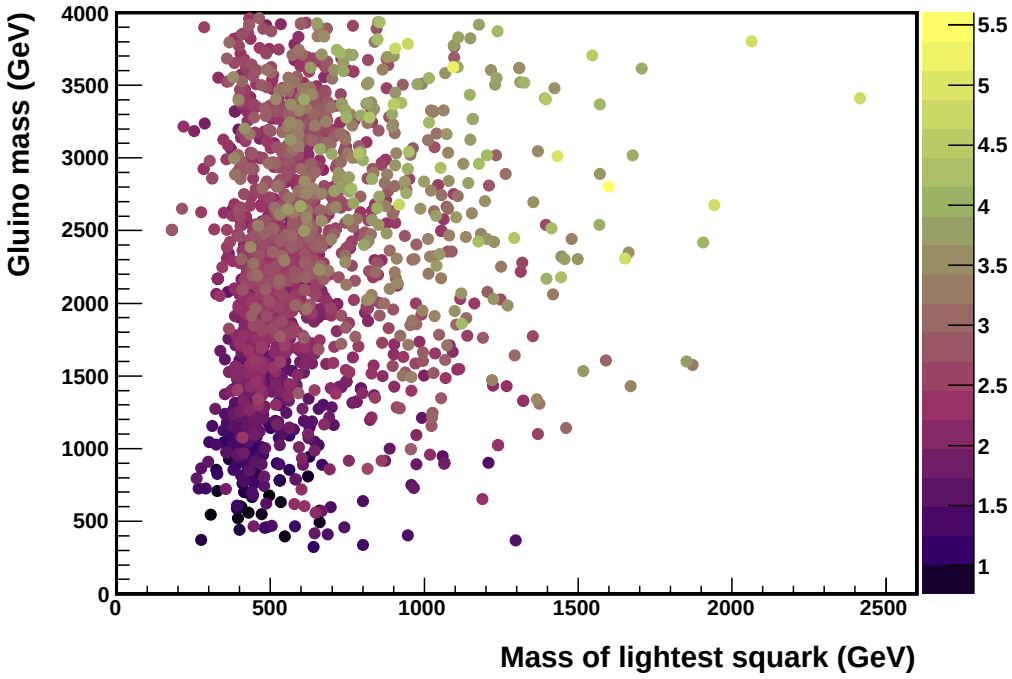

Figure 5: $\log_{10}$[luminosity $(\text{pb})^{-1}$ needed for discovery] in the $(m_{\tilde{g}}, m_{\text{lightest } \tilde{q}})$ plane at 14 TeV with a combination of the MET based and optimised M_{T2} based strategies. The M_{T2} based strategy was optimized for an integrated luminosity of 1 fb^{-1}. Systematic uncertainties in the background have been neglected.

the lightest sparton on the abscissa, some points are still much harder to discover than others. The variation of luminosity with Δm suggests that another important factor for discoverability is the mass degeneracy of the lightest sparton and the LSP.

A few representative spectra of hard-to-discover points are shown in figure 7, as plotted with `PySLHA` [23]. We identified 57 points which require more than 10 fb^{-1} at $\sqrt{s} = 14$ TeV to be discovered. Several categories can be distinguished:

1) Points which due to high sparton masses have a small sparton production cross-section of less than 10 fb, while the overall SUSY cross-section is above 10 fb due to slepton and gaugino production. These points cannot be easily discovered at the LHC with any of the ATLAS MET search strategies unless dedicated studies [24, 25] are employed. These points might be easier to discover at a future linear collider. A representative mass spectrum of the 16 points identified in this category is shown in figure 7a.

2) Points which due to the high sparticle masses have a small overall production cross-section of less than 10 fb. These points might prove difficult to discover at a future linear collider as well. A representative mass spectrum of the 15 points that fall in this category is shown in figure 7b.

3) Points which are not cross-section limited, i.e. $\sigma > 10$ fb.

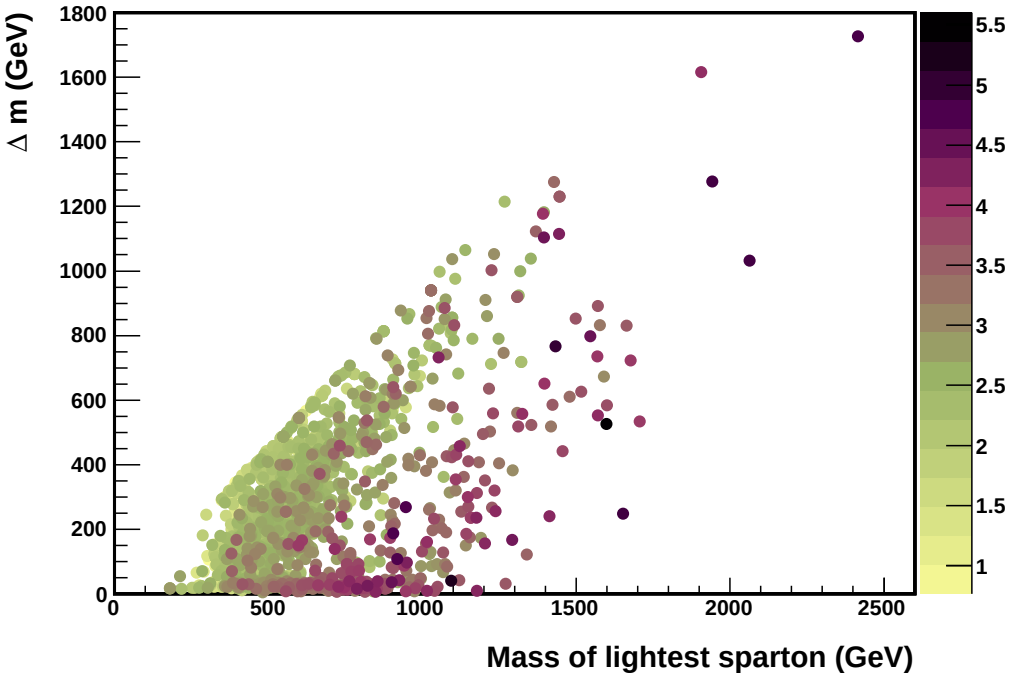

Figure 6: $\log_{10}$[luminosity $(\text{pb})^{-1}$ needed for discovery] with the combined optimal M_{T2} and MET based strategy at $\sqrt{s} = 14$ TeV in the $(\Delta m, m_{\text{lightest sparton}})$ plane. Δm is the mass difference between the lightest sparton and the LSP. The M_{T2} based strategy was optimized for an integrated luminosity of 1 fb^{-1}. Systematic uncertainties in the background have been neglected.

The above three categories are mutually exclusive. However, the points can also be categorised depending on the mass degeneracies of the lightest sparton and the LSP, and we show such spectra in figures 7c, 7d. Any other squarks and the gluino are far more massive and their production is therefore suppressed. Even if the production cross-section for the nearly mass-degenerate squarks is large enough, above 10 fb, the mass degeneracy leads to a decay topology which only gives soft jets, making the signal difficult to distinguish from background. We identified in our sample 16 points which have a lightest squark of the first two generations nearly mass-degenerate with the LSP and 7 points which have a $\tilde{b}$ or $\tilde{t}$ squark nearly mass-degenerate with the LSP. 6 points fall in both categories, having both the lightest squark of the first two generations and the lightest squark of the third generation nearly mass-degenerate with the LSP. Points with mass near-degenerate particles could be dealt with by looking at events where the produced sparticle pair is boosted by the emission of hard-QCD jets from initial or final state radiation [26, 27].

Five hard-to-discover points are both cross-section limited and exhibit large mass degeneracies, which will make them particularly hard to tackle at the LHC.

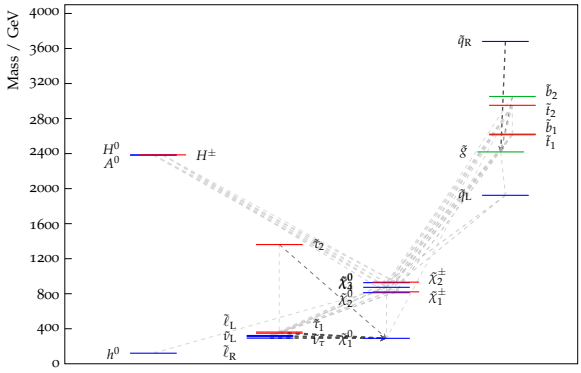

(a) An example of a point where all squarks and the gluino are very heavy. Gaugino production dominates. (16 such points identified).

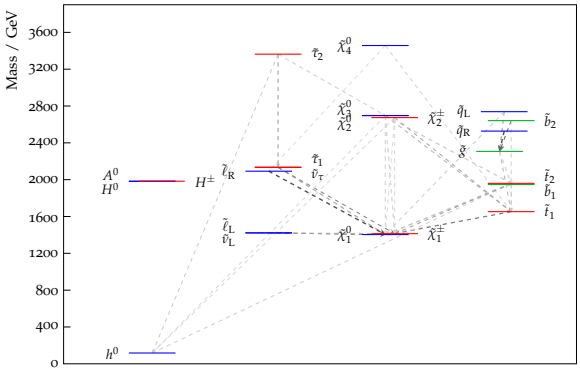

(b) An example of a point where all sparticles are very heavy (15 such points identified).

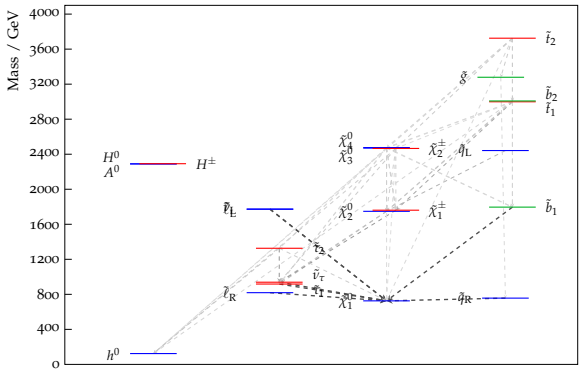

(c) An example of a point with nearly mass-degenerate squark of the first two generations and LSP (16 points identified).

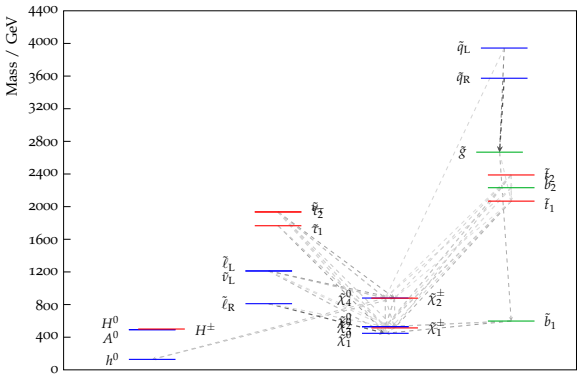

(d) An example of a point with nearly mass-degenerate squark of the third generation and LSP (7 points identified).

Figure 7: Some hard to discover points. The dotted lines show possible decay modes. Only branching ratios of above 5% have been drawn. The darker shades correspond to higher branching ratios.

11 Discussion

Recent papers by Conley et al. [8, 9] describe similar studies to the present one, applying several other ATLAS MET based search strategies on a set of ∼71k model points in pMSSM. The similarities and differences between these studies and ours are discussed in this section.

In the scenarios studied by Conley et al., an additional particle outside the MSSM is implicitly assumed to make up part or all of the dark matter relic density. This has the consequence of a preponderance of wino dominated lightest supersymmetric particles, leading to quasi-mass degenerate lightest charginos and lightest neutralinos. Reference [9] did not perform a global fit, but instead scanned for points which were compatible with each experimental 95% CL. Depending on the scan prior used, the sparticle masses were constrained to be less than 3 TeV or 1 TeV. Each point was given equal weight in their results.

In comparison to our work, in the MET based strategies employed by Conley et al., the lepton multiplicity required is varied. However, it is suggested both in their work and in ATLAS studies [1, 3] that the 0 lepton channel is the most robust of the MET-based analyses. The backgrounds in references [8, 9] were produced by the ATLAS SUSY group with state-of-the-art Monte Carlo event generators and the full ATLAS detector simulation. The signal was generated using a fast detector simulation.

For different scenarios with systematic uncertainty in the background of 50% or 20%, Conley et al. calculate how many of the generated SUSY points are discoverable using any of the ATLAS 11 MET analyses, requiring the same criteria for discoverability as the ones in the present paper. Conley et. al found an optimal cut on the value of the $M_{\rm eff}$ variable employed in MET type analyses, while we did the same for the M_{T2} variable. It is difficult to perform a direct analysis between our results and those by Conley et al., since their paper starts out from different assumptions. We note for example that setting the sparticle mass upper range to 1 or 3 TeV would have further increased the fraction of points discovered in our study.

Reference [9] found that, at $\sqrt{s} = 7$ TeV and after 1 fb^{-1}, MET cuts would discover between 50-90% of the models considered, depending on the systematic error assumed on the background. Here, we found a similar level of dependence of M_{T2}-based search discoverability on the systematic error assumed. References [8, 9] did not consider the M_{T2} based search strategy.

Conley et al. also study the effect of a detector-stable charged LSP, whereas the LSP in the points we investigated was $\tilde{\chi}_1^0$ throughout. We did find though 7 points with pseudo-stable $\tilde{\chi}_1^+$, 1 point with pseudo-stable $\tilde{\chi}_2^0$ and 13 points with pseudo-stable $\tilde{\tau}_1$.[d] These points exhibit extreme mass degeneracies between the pseudo-stable, next-to-lightest supersymmetric particle and the LSP. The mass difference is a few hundred MeV and the decay is strongly phase-space suppressed. The pseudo-stable particles have decay lengths from a few centimeters to several meters. Whilst the simulation that we performed becomes invalid for these points since it includes no information on the detector geometry, the high production cross-section for these points combined with a search for long-lived charged particles would make such points detectable by other means [1].

The analysis of the discovery reach of a search strategy based on M_{T2} is unique to our paper. Also, in our study we have taken into consideration a bigger range of sparticle masses, allowing for much higher hierarchies in the points studied. The limited range of sparticle masses restricts the type of hard-to-discover points found by references [8, 9]. Both our study and references [8, 9] investigated the effects of varying the systematic uncertainty in the background and the luminosity, but Conley et al. did not explore the discovery potential at $\sqrt{s} = 14$ TeV for luminosities higher than 1 fb^{-1}, a luminosity which will certainly be surpassed at the LHC.

[d] We consider a particle to be "pseudo-stable" if it has a lifetime larger than 100 picoseconds or equivalently its decay length is longer than 3 cm.

12 Conclusions

We have simulated searches for SUSY at the LHC, assuming different luminosities and centre of mass energies. We used a selection based on the M_{T2} variable alone, an ATLAS MET-type search strategy and a combined approach and applied them to ∼2000 pMSSM good-fit points. Based on these we have suggested optimal values for the cut on M_{T2} for low luminosities, which are 320 GeV for $\sqrt{s} = 7$ TeV and 400 GeV for $\sqrt{s} = 14$ TeV.

Ignoring systematic uncertainties in the background and using a combined optimised M_{T2} and MET based search, we reach the following conclusion. If we assign equal probability to each model studied, a 7 TeV LHC would discover SUSY with 42.5% probability after accumulating 10 fb^{-1}. Similarly, a 14 TeV LHC would discover SUSY in 96.1% of the cases after an integrated luminosity of 10 fb^{-1}. The few points that still evade detection are characterised by heavy gluino masses above 2.5 TeV and heavy squark masses or high mass degeneracies between the lightest squark and the LSP.

The M_{T2} based strategy is better suited than the MET based strategy for integrated luminosities up to several inverse femtobarns, in the absence of systematic uncertainties in the background. The M_{T2} strategy is based on a single cut on M_{T2}. It accepts both more signal and more background than the MET strategy, meaning that at higher luminosities it is more vulnerable to fixed fractional systematic uncertainties in the background. The MET based strategy is more sensitive than the M_{T2} based strategy to points with high gluino masses. Of course, a combined strategy is the most powerful.

An optimization of the standard ATLAS searches (i.e. finding optimal values for the cuts on the selection variables used therein) would be desirable, though more difficult to make, due to the multi-dimensionality of the parameter space. A further optimization only makes sense in the context of good understanding of the systematic uncertainties, an important concern for the experiments.

While the LHC machine and the ATLAS and CMS experiments have performed remarkably well, SUSY searches at the LHC are still in their infancy. Our work suggests that there is still much more of the parameter space to be explored and that this can be done efficiently using the search strategies available.

Acknowledgments

We are grateful to the authors of [10] for providing us with the points analysed. Sasha Caron has kindly provided the significance calculator for section 8. A.D. is thankful to Merton College, Oxford for hospitality. This work has been partially supported by STFC.

References

[1] **The ATLAS** Collaboration, G. Aad *et. al.*, *Expected Performance of the ATLAS Experiment - Detector, Trigger and Physics*, hep-ex/0901.0512.

[2] G. L. Bayatian *et. al.*, *CMS physics Technical Design Report, Volume II: Physics Performance. oai:cds.cern.ch:942733*, *J. Phys. G* **34** (2006), no. CERN-LHCC-2006-021. CMS-TDR-008-2 995–1579. 669 p.

[3] **The ATLAS** Collaboration, G. Aad *et. al.*, *Search for squarks and gluinos using final states with jets and missing transverse momentum with the ATLAS detector in sqrt(s) = 7 TeV proton-proton collisions*, hep-ex/1102.5290.

[4] **CMS** Collaboration, V. Khachatryan *et. al.*, *Search for Supersymmetry in pp Collisions at 7 TeV in Events with Jets and Missing Transverse Energy*, hep-ex/1101.1628.

[5] C. G. Lester and D. J. Summers, *Measuring masses of semiinvisibly decaying particles pair produced at hadron colliders*, *Phys. Lett.* **B463** (1999) 99–103, [hep-ph/9906349].

[6] A. Barr, C. Lester, and P. Stephens, *m(T2) : The Truth behind the glamour*, *J. Phys.* **G29** (2003) 2343–2363, [hep-ph/0304226].

[7] A. J. Barr and C. Gwenlan, *The race for supersymmetry: using M_{T2} for discovery*, *Phys. Rev.* **D80** (2009) 074007, [hep-ph/0907.2713].

[8] J. A. Conley, J. S. Gainer, J. L. Hewett, M. P. Le, and T. G. Rizzo, *Supersymmetry Without Prejudice at the LHC*, hep-ph/1009.2539.

[9] J. A. Conley, J. S. Gainer, J. L. Hewett, M. P. Le, and T. G. Rizzo, *Supersymmetry Without Prejudice at the 7 TeV LHC*, hep-ph/1103.1697.

[10] S. S. AbdusSalam, B. C. Allanach, F. Quevedo, F. Feroz, and M. Hobson, *Fitting the Phenomenological MSSM*, *Phys. Rev.* **D81** (2010) 095012, [hep-ph/0904.2548].

[11] F. Feroz and M. P. Hobson, *Multimodal nested sampling: an efficient and robust alternative to MCMC methods for astronomical data analysis*, astro-ph/0704.3704.

[12] F. Feroz, M. P. Hobson, and M. Bridges, *MultiNest: an efficient and robust Bayesian inference tool for cosmology and particle physics*, astro-ph/0809.3437.

[13] B. C. Allanach *et. al.*, *The Snowmass points and slopes: Benchmarks for SUSY searches*, *Eur. Phys. J.* **C25** (2002) 113–123, [hep-ph/0202233].

[14] **The ATLAS** Collaboration, G. Aad *et. al.*, *Prospects for Supersymmetry discovery based on inclusive searches at a 7 TeV centre-of-mass energy with the ATLAS detector*, Tech. Rep. ATL-PHYS-PUB-2010-010, CERN, Geneva, Jul, 2010.

[15] H.-C. Cheng and Z. Han, *Minimal Kinematic Constraints and MT2*, *JHEP* **12** (2008) 063, [hep-ph/0810.5178].

[16] **The ATLAS** Collaboration, G. Aad *et. al.*, *Early supersymmetry searches in channels with jets and missing transverse momentum with the ATLAS detector*, Tech. Rep. ATLAS-CONF-2010-065, CERN, Geneva, Jul, 2010.

[17] M. Bahr *et. al.*, *Herwig++ Physics and Manual*, *Eur. Phys. J.* **C58** (2008) 639–707, [arXiv:0803.0883].

[18] S. Gieseke *et. al.*, *Herwig++ 2.5 Release Note*, hep-ph/1102.1672.

[19] P. Z. Skands *et. al.*, *SUSY Les Houches Accord: Interfacing SUSY Spectrum Calculators, Decay Packages, and Event Generators*, *JHEP* **07** (2004) 036, [hep-ph/0311123].

[20] M. Cacciari and G. P. Salam, *Dispelling the N^3 myth for the k_t jet-finder*, *Phys. Lett.* **B641** (2006) 57–61, [hep-ph/0512210].

[21] M. Cacciari, G. P. Salam, and G. Soyez, *The anti-k_t jet clustering algorithm*, *JHEP* **04** (2008) 063, [hep-ph/0802.1189].

[22] R. D. Cousins, J. T. Linnemann, and J. Tucker, *Evaluation of three methods for calculating*

statistical significance when incorporating a systematic uncertainty into a test of the background-only hypothesis for a Poisson process, *Nucl. Instrum. Meth.* **A595** (2008) 480–501.

[23] A. Buckley. http://www.insectnation.org/projects/pyslha.

[24] E. Lytken, *Searches for Direct Slepton Production with ATLAS*, *Czech.J.Phys.* **54** (2004) A169–A173.

[25] C.-Y. Chen and A. Freitas, *General analysis of signals with two leptons and missing energy at the Large Hadron Collider*, *JHEP* **1102** (2011) 002, [hep-ph/1011.5276].

[26] D. S. M. Alves, E. Izaguirre, and J. G. Wacker, *Where the Sidewalk Ends: Jets and Missing Energy Search Strategies for the 7 TeV LHC*, hep-ph/1102.5338.

[27] J. Alwall, M.-P. Le, M. Lisanti, and J. G. Wacker, *Searching for Directly Decaying Gluinos at the Tevatron*, *Phys. Lett.* **B666** (2008) 34–37, [hep-ph/0803.0019].